

# Effect of the next-nearest neighbor hopping on the stability and band structure of the incommensurate phases in the cuprates

Marcin Raczkowski<sup>\*1</sup>, Raymond Frésard<sup>2</sup>, and Andrzej M. Oleś<sup>1,3</sup>

<sup>1</sup> Marian Smoluchowski Institute of Physics, Jagellonian University, Reymonta 4, 30059 Kraków, Poland

<sup>2</sup> Laboratoire CRISMAT, UMR CNRS-ENSICAEN 6508, 6 Bld. du Maréchal Juin, 14050 Caen, France

<sup>3</sup> Max-Planck-Institut für Festkörperforschung, Heisenbergstrasse 1, 70569 Stuttgart, Germany

Received , revised , accepted

Published online

**Key words** stripe phase, spiral phase, band structure, Hubbard model, doped cuprates.

**PACS** 71.10.Fd, 71.27.+a, 74.72.-h

Using a spin-rotation invariant version of the slave-boson approach we investigate the relative stability and band structure of various incommensurate phases in the cuprates. Our findings obtained in the Hubbard model with next-nearest neighbor hopping  $-t'/t \simeq 0.15$ , as appropriate for the  $\text{La}_{2-x}\text{Sr}_x\text{CuO}_4$  family, support the formation of diagonal (vertical) stripe phases in the doping regime  $x = 1/16$  ( $x = 1/8$ ), respectively. In contrast, based on the fact that a larger value  $-t'/t = 0.3$  expected for  $\text{YBa}_2\text{Cu}_3\text{O}_{6+\delta}$  triggers a crossover to the diagonal (1,1) spiral phase at increasing doping, we argue that it might explain why the static charge order has been detected in  $\text{YBa}_2\text{Cu}_3\text{O}_{6+\delta}$  only in the highly underdoped regime.

Copyright line will be provided by the publisher

The abundance of experimental results and theoretical investigations in recent years have shown that the ground state of the high- $T_c$  cuprates might be spatially inhomogeneous [1]. In particular, both charge and spin modulations have been detected in neutron scattering studies performed on  $\text{La}_{1.6-x}\text{Nd}_{0.4}\text{Sr}_x\text{CuO}_4$ . Remarkably, incommensurate (IC) Bragg peaks indicate that in the lightly doped regime  $x < 1/16$  the antiferromagnetic (AF) domains are separated by *diagonal* charge domain walls (DWs) [2] but at a higher doping level  $x = 1/8$  the doped holes self-organize into stripes that run *vertically* across the  $\text{CuO}_2$  planes [3]. On the one hand, the former are on average filled by  $1/\sqrt{2}$  hole per two DWs or even by one hole per one atom in a DW as established in  $\text{La}_{2-x}\text{Sr}_x\text{CuO}_4$  (LSCO) around  $x = 0.02$  [4], which corresponds to the so-called *filled* stripes. On the other hand, the latter are characterized by the filling of one hole per two atoms along the DWs meaning that they are only *half-filled*. IC charge order consistent with vertical/horizontal stripes has also been reported in highly underdoped  $\text{YBa}_2\text{Cu}_3\text{O}_{6+\delta}$  (YBCO) with  $\delta = 0.35$  [5], but despite several attempts no static charge order could have been detected at higher doping. Apart from explaining the neutron scattering data, stripe phases also offer a framework for interpreting a broad range of other experimental results such as angle-resolved photoemission spectroscopy (ARPES) [6] (see below) as well as magnetic excitation spectra in both LSCO and YBCO families that might be consistently explained in terms of fluctuating stripes [7, 8].

While the stripe debate continues, an alternative scenario which might account for the IC spin structure in LSCO is a deformation of the AF order so as to optimize the hole motion that stabilizes a spiral phase [9, 10]. Moreover, Lindgård [11] has shown that spiral states can also resolve the universality of magnetic excitations in the cuprates and provide a competing paradigm with the stripe phase concept. Therefore, the main purpose of this paper is to address in a systematic way the competition between two possible *site-centered* (i.e., with a fully suppressed magnetization along the domain walls) stripe ground states: half-filled vertical site-centered (HVSC) and filled diagonal site-centered (FDSC), their *bond-centered*

\* Corresponding author: e-mail: M.Raczkowski@if.uj.edu.pl, Phone: +48 12 663 5628, Fax: +48 12 633 4079

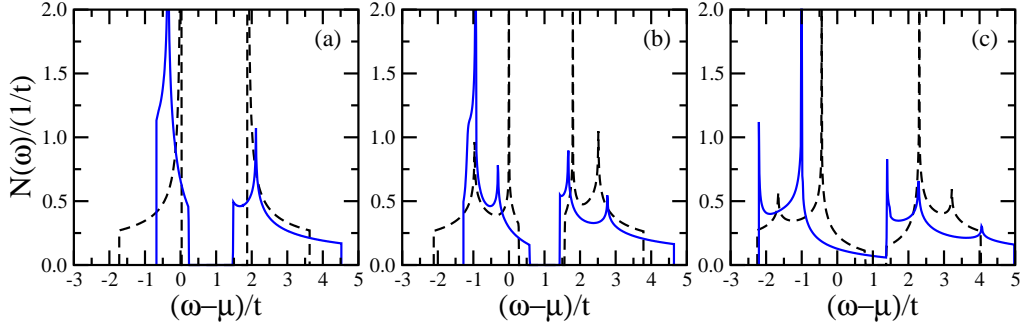


**Fig. 1** Effect of the next-nearest neighbor hopping  $t'$  on the density of states at doping  $x = 1/8$  as obtained in the extended Hubbard model for the uniform: (a) AF phase; (b) (0,1) spiral phase, and (c) (1,1) spiral phase. Parameters:  $U = 12t$ ,  $t' = 0$  (dashed line), and  $t' = -0.3t$  (solid line).

counterparts (where DWs are given by ladders with a weak ferromagnetic order on the rungs): half-filled vertical bond-centered (HVBC) and filled diagonal bond-centered (FDBC) DWs, as well as between the vertical (0,1) and diagonal (1,1) spiral phases. In order to treat noncanted stripe phases and the spiral order on equal footing and to implement local electron correlations we employ a rotationally invariant version of the slave-boson (SB) approach in spin space [12] by introducing auxiliary boson operators  $\{e_i, d_i, p_{i0}, \mathbf{p}_i\}$  which control the actual electronic configuration at each site  $i$ . The Hamiltonian may be then written as,

$$H = - \sum_{ij} \sum_{\sigma\lambda\tau} t_{ij} z_{i\sigma\lambda}^\dagger f_{i\lambda}^\dagger f_{j\tau} z_{j\tau\sigma} + U \sum_i d_i^\dagger d_i, \quad (1)$$

where  $\{z_i, z_j\}$  are  $2 \times 2$  matrices in spin space which depend on the actual configuration of the boson fields, the hopping  $t_{ij}$  is  $t$  on the bonds connecting nearest-neighbor sites and  $t'$  for next-nearest neighbor sites, while  $U$  is the on-site Coulomb interaction. Calculations were carried out on square  $128 \times 128$  clusters which became possible by developing an efficient scheme in reciprocal space which makes use of the stripe symmetry [13]. In our studies, we have chosen  $U = 12t$ , which gives the ratio of  $J/t = 1/3$  (with the superexchange  $J = 4t^2/U$ ), being a value representative for LSCO [14].

Regarding the excitation spectrum of the Hubbard model, dynamical mean-field theory (DMFT) revealed that it consists of a lower Hubbard band (LHB), an upper Hubbard band (UHB), and a quasiparticle peak that vanishes at the Mott transition [16]. Since the former two are dynamical in nature, they are hardly present in mean-field calculations, while the latter is at the heart of the Brinkman-Rice description of the Mott transition and of the equivalent SB mean-field approach in the paramagnetic phase. In contrast, in stripe phases bands, separated by energies of order  $U$  and corresponding to the LHB and UHB, are part of the spectrum, on top of midgap bands in which the chemical potential may be located, as discussed below.

Let us now review the mechanisms responsible for the stability of these various IC phases in the pure Hubbard model with  $t' = 0$  at moderate doping  $x < 0.15$ . First of all, Fig. 1 shows that a prominent

**Table 1** Local magnetization  $m_i$  and double occupancy  $d_i$  as found for the uniform AF state as well as for (0,1) and (1,1) spiral phases in the extended Hubbard model with  $U = 12t$  for  $x = 1/16$ , and  $x = 1/8$ .

phase	$x = 1/16$				$x = 1/8$			
	$t' = 0$	$t'/t = -0.3$	$t' = 0$	$t'/t = -0.3$	$m_i$	$d_i$	$m_i$	$d_i$
AF	0.803	0.0265	0.799	0.0257	0.586	0.0227	0.595	0.0207
(0,1)	0.813	0.0257	0.811	0.0247	0.646	0.0216	0.656	0.0190
(1,1)	0.820	0.0251	0.829	0.0229	0.682	0.0202	0.730	0.0158

**Table 2** Free energy  $F/t$  per site for various phases at  $x = 1/8$  found in the SB approximation in the extended Hubbard model with  $U = 12t$  for representative values of the next-nearest neighbor hopping:  $t' = 0$ ,  $t' = -0.15t$ , and  $t' = -0.3t$ . The most advantageous energy for each  $t'$  is given in bold characters.

$t'/t$	AF	(0,1)	(1,1)	FDSC	FDBC	HVSC	HVBC
0.00	-0.5393	-0.5613	-0.5700	<b>-0.5821</b>	-0.5819	-0.5689	-0.5680
-0.15	-0.5323	-0.5564	-0.5699	<b>-0.5716</b>	-0.5713	-0.5700	-0.5691
-0.30	-0.5341	-0.5594	<b>-0.5842</b>	-0.5655	-0.5651	-0.5749	-0.5740

feature of the spiral phases is the van Hove singularity below the Fermi energy that leads to a substantial energy gain with respect to the AF phase. Remarkably, this energy gain is amplified by doping making the spiral phases increasingly competitive. Next, as listed in Table 1, they are characterized by larger staggered magnetization resulting into smaller double occupancy and consequently into a better Coulomb energy as compared to the AF phase. Finally, one finds that this mechanism is more effective when the spiral twist is along the diagonal of the Brillouin zone. In contrast, stripe phases result from a compromise between the optimized kinetic energy of doped holes and the superexchange interaction [13]. Indeed, propagation of doped holes is easy when the magnetization is locally suppressed along the charge DWs, while the superexchange is best optimized when the AF domains are close to half-filling.

Turning now to the extended Hubbard model, the main effect of  $t'$  is to shift the van Hove singularity towards negative energy [15]. As a result, perfect nesting of the Fermi surface is broken and a metal-to-insulator transition occurs for a finite  $U_c$ , even at half-filling [17]. Accordingly, antiferromagnetism is suppressed at  $x = 0$  becoming, however, enhanced when moving towards the van Hove point. Similarly, the filled stripe phases should not benefit from  $t'$  as it strongly frustrates the antiferromagnetism in the weakly doped AF domains separating DWs. In contrast, one can conjecture that the spiral phases better make use of the van Hove singularity by its systematic shift below the Fermi energy. This, together with both larger staggered magnetization and smaller double occupancy, should yield a more significant energy gain and make the spiral phases more competitive with increasing  $-t'/t$ . Therefore, one may expect a critical  $t'$  for which the (1,1) spiral phase becomes the ground state. As shown in Table 2, this indeed happens for  $t' \simeq -0.2t$  at doping  $x = 1/8$ . In this case, one observes a spectacular transfer of density of states from the Fermi energy towards the bottom of the LHB as depicted in Fig. 1(c). In addition, staggered magnetization in the (1,1) spiral phase is strongly enhanced as compared to the AF phase supported by concomitant reduction of double occupancy (see Table 1). However, Table 3 shows that for small doping  $x = 1/16$ , the above mechanisms are not sufficient to stabilize the spiral order even for  $t'/t = -0.3$ .

Remarkably, since the holes are more delocalized over the AF domains which are then less frustrated, finite  $t'$  also promotes the half-filled vertical stripe phase. In addition, it induces conspicuous changes in the band structure that should have measurable consequences in ARPES experiments. First of all, as shown in Fig. 2(a) segregation of doped holes into *metallic* site-centered DWs gives rise to the appearance of two additional *partially* filled bands lying within the Mott-Hubbard gap. Secondly, as a consequence of the vertical stripe order, the  $\Gamma - X$  and  $\Gamma - Y$  directions with  $X = (\pi, 0)$  and  $Y = (0, \pi)$  are inequivalent. Indeed, as the fully quenched spin polarization facilitates the propagation of the holes along the site-centered DWs, the maximum dispersion is expected along the  $\Gamma - Y$  direction. In contrast, the midgap bands almost do not disperse along the  $\Gamma - X$  direction, which indicates that the holes are rather static along the

**Table 3** The same as in Table 2 but for  $x = 1/16$ . FDBC stripe phase is unstable at  $t' = -0.3t$ .

$t'/t$	AF	(0,1)	(1,1)	FDSC	FDBC	HVSC	HVBC
0.00	-0.4183	-0.4286	-0.4363	<b>-0.4561</b>	-0.4560	-0.4496	-0.4492
-0.15	-0.4173	-0.4287	-0.4376	<b>-0.4508</b>	-0.4507	-0.4503	-0.4499
-0.30	-0.4194	-0.4319	-0.4444	-0.4478	-	<b>-0.4529</b>	-0.4525

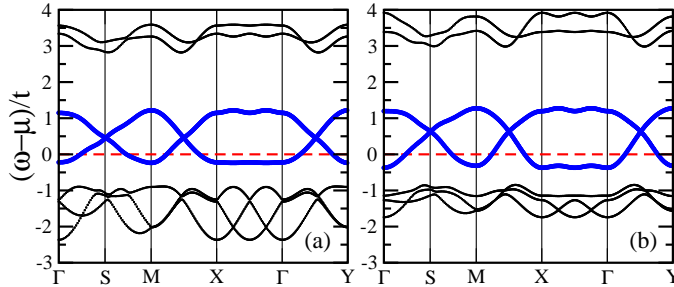


**Fig. 2** Low energy part of the electronic structure found at  $x = 1/8$  for the HFSC stripe phase in the extended Hubbard model with  $U = 12t$  as well as with: (a)  $t' = 0$  and (b)  $t' = -0.15t$ . Thick solid line depicts midgap states while dashed line indicates the Fermi level. The highest energy band is centered around  $\omega - \mu \simeq 7t$ .

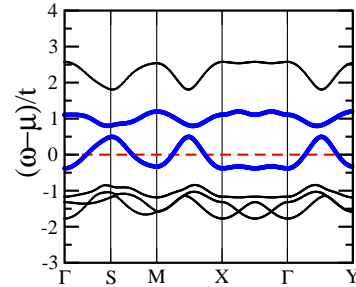


**Fig. 3** The same as in Fig. 2(b) but for the HVBC stripe phase. The two highest energy bands are centered around  $\omega - \mu \simeq 6t$ .

horizontal direction. Therefore, both midgap bands could be approximated by one-dimensional noninteracting dispersion  $\epsilon_{\mathbf{k}}^{\text{DW}} = \pm 2t \cos k_y + \text{cst}$ . It crosses the Fermi energy  $\mu$  at  $\mathbf{k} = (\pi, \pi/4), (\pi/4, \pi/4)$ , and at the equivalent points as expected for the stripes separated by four lattice spacings. However, due to strong local correlations the bandwidth of these states is strongly renormalized and reduced down to  $W_{\text{DW}}/t \simeq 1.45$ . On the one hand, some features depicted in Fig. 2(a) such as the flat band near the  $X$  point crossing the Fermi level at the  $\mathbf{k} = (\pi, \pi/4)$  point and excitations at the  $S = (\pi/2, \pi/2)$  point at a higher binding energy than at the  $X$  point, are in a close agreement with the ARPES spectral density for LSCO at  $x = 1/8$  [6]. On the other hand, no spectral weight was found at the Fermi energy along the nodal  $\Gamma - M$  direction with  $M = (\pi, \pi)$ , especially at the  $(\pi/4, \pi/4)$  point. Therefore, one has to use more accurate methods, such as the DMFT, which include dynamical correlations and leads to a better agreement with the experimental data, reproducing a pseudogap at  $x = 1/8$  [14]. Furthermore, Fig. 2(b) indicates that a negative  $t' = -0.15t$ , as expected for LSCO, leads to a distinct broadening of the midgap bandwidth up to  $W_{\text{DW}}/t \simeq 1.6$ . Consequently, it shifts these states to a lower energy which explains the increasing stability of the half-filled DWs in spite of the concomitant narrowing of the LHB bandwidth associated with the insulating AF background. Finally, similar conclusions might be drawn concerning the effect of  $t'$  on the band structure of the HVBC stripe phase shown in Fig. 3. In this case, one finds a gap between both midgap states due to a finite AF spin polarization along the bond-centered DWs.

An entirely different mechanism is responsible for the stability of the *filled* site-centered DWs. It might be best understood from the band structure shown for  $x = 1/16$  in Fig. 4(a). Here, each diagonal DW induces the formation of two (dispersionless along the  $X - Y$  direction) entirely *unoccupied* midgap bands. Thus the special stability of these phases follows from a real gap that opens in the symmetry broken state between the highest occupied state of the LHB and the bottom of the midgap band [18, 19]. Besides, the main effect of increasing  $-t'/t$  is to narrow the LHB and to push its lowest energy states towards higher energy while the midgap states remain intact as depicted in Fig. 4(b). This feature is clearly visible along the parallel to the stripes  $\Gamma - M$  direction and strongly decreases the stability of the FDSC stripe phase with respect to the half-filled one (see Tables 2 and 3). Unfortunately, the above gap and the resulting insulating character is inconsistent with the ARPES data on the lightly doped LSCO. Indeed, experimentally a quasiparticle peak crosses the Fermi level in the nodal direction  $\Gamma - M$  and forms a hole pocket at the  $S$  point [20]. A possible interpretation, obtained on the Hartree-Fock level by Granath [21], is provided by Fig. 5 showing that finite spectral weight around the  $S$  point may arise from the bond-centered DWs explaining naturally the metallic behavior at high temperatures of the lightly doped LSCO. In this case, finite spin polarization of DWs leads to the hybridization of the midgap bands with the LHB. Such feature was also found in the two-band Hubbard model describing stripe phases in the nickelates [22].

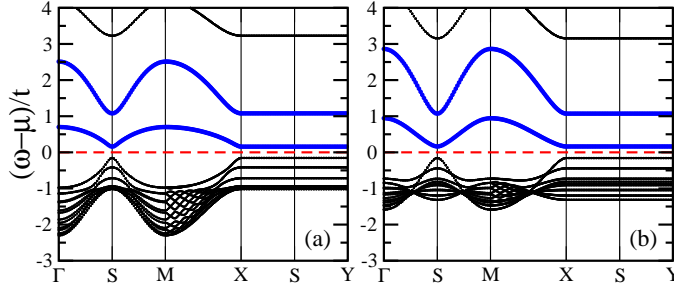


**Fig. 4** Low energy part of the electronic structure found at  $x = 1/16$  for the FDSC stripe phase in the extended Hubbard model with  $U = 12t$  as well as with: (a)  $t' = 0$  and (b)  $t' = -0.15t$ . The highest energy bands (not shown) are centered around  $\omega - \mu \simeq 9t$ .

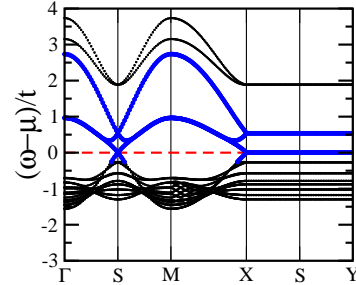


**Fig. 5** The same as in Fig. 4(b) but for the FDBC stripe phase. The highest energy bands (not shown) are centered around  $\omega - \mu \simeq 9t$ .

In conclusion, we have found that the next-nearest neighbor hopping  $t'$  plays an important role in affecting the relative stability and the band structure of the IC phases. Next, partial filling of the bands within the Mott-Hubbard gap, pseudogap that forms at the Fermi energy around the  $S$  point, and the flat band near the  $X$  point crossing the Fermi level at the  $\mathbf{k} = (\pi, \pi/4)$  point are found to be general consequences of the half-filled vertical stripe phase in qualitative agreement with the ARPES results established at doping  $x = 1/8$ . In contrast, finite spectral weight around the  $S$  point experimentally observed at  $x = 1/16$  doping might be attributed to the FDBC stripe phase also explaining the metallic behavior of the lightly doped LSCO. Finally, we would like to emphasize that the strongly enhanced stability of the (1,1) spiral phase by finite  $t'$  above  $x = 1/8$  with respect to the above stripe phases is robust and is not affected even by optimizing the stripe filling that further lowers the energy of the stripe phases [23]. This may explain why the static charge order has been detected in  $\text{YBa}_2\text{Cu}_3\text{O}_{6+\delta}$  only in the highly underdoped regime.

**Acknowledgements** This work was supported by the Polish Ministry of Science and Education under Project No. 1 P03B 068 26 and by the Ministère Français des Affaires Etrangères under POLONIUM 09294VH.

## References

- [1] S. A. Kivelson *et al.*, Rev. Mod. Phys. **75**, 1201 (2003).
- [2] S. Wakimoto *et al.*, Phys. Rev. B **64**, 174505 (2001).
- [3] J. M. Tranquada, B. J. Sternlieb, J. D. Axe, Y. Nakamura, and S. Uchida, Nature **375**, 561 (1995).
- [4] M. Fujita *et al.*, Phys. Rev. B **65**, 064505 (2002).
- [5] H. A. Mook, P. Dai, and F. Doğan, Phys. Rev. Lett. **88**, 097004 (2002).
- [6] A. Damascelli, Z. Hussain, and Z.-X. Shen, Rev. Mod. Phys. **75**, 473 (2003).
- [7] G. Seibold and J. Lorenzana, Phys. Rev. Lett. **94**, 107006 (2005).
- [8] M. Vojta, T. Vojta, and R. K. Kaul, Phys. Rev. Lett. **97**, 097001 (2006).
- [9] R. Frésard, M. Dzierzawa, and P. Wölfle, Europhys. Lett. **15**, 325 (1991).
- [10] N. Hasselmann, A. H. Castro Neto, and C. Morais Smith, Phys. Rev. B **69**, 014424 (2004).
- [11] P.-A. Lindgård, Phys. Rev. Lett. **95**, 217001 (2005).
- [12] W. Zimmermann, R. Frésard, and P. Wölfle, Phys. Rev. B **56**, 10097 (1997).
- [13] M. Raczkowski, R. Frésard, and A. M. Oleś, Phys. Rev. B **73**, 174525 (2006).
- [14] M. Fleck, A. I. Lichtenstein, and A. M. Oleś, Phys. Rev. B **64**, 134528 (2001).
- [15] M. Fleck, A. M. Oleś, and L. Hedin, Phys. Rev. B **56**, 3159 (1997).
- [16] A. Georges, G. Kotliar, W. Krauth, and M. J. Rozenberg, Rev. Mod. Phys. **68**, 13 (1996).
- [17] I. Yang, E. Lange, and G. Kotliar, Phys. Rev. B **61**, 2521 (2000).
- [18] J. Zaanen and A. M. Oleś, Ann. Phys. (Leipzig) **5**, 224 (1996).
- [19] M. Ichioka and K. Machida, J. Phys. Soc. Jpn. **68**, 4020 (1999).
- [20] T. Yoshida *et al.*, Phys. Rev. Lett. **91**, 027001 (2003).
- [21] M. Granath, cond-mat/0603156 (unpublished).
- [22] M. Raczkowski, R. Frésard, and A. M. Oleś, Phys. Rev. B **73**, 094429 (2006).
- [23] M. Raczkowski, R. Frésard, and A. M. Oleś (unpublished).